Biochimica et Biophysica Acta 1840 (2014) 1701–1711

Contents lists available at ScienceDirect

Biochimica et Biophysica Acta

journal homepage: www.elsevier.com/locate/bbagen

Cloning, characterization, and expression of glucose transporter 2 in the freeze-tolerant wood frog, *Rana sylvatica*

Andrew J. Rosendale [a,*], Benjamin N. Philip [b], Richard E. Lee Jr. [a], Jon P. Costanzo [a]

[a] Department of Zoology, Miami University, 700 E. High St., Oxford, OH 45056, USA
[b] Department of Biology, Rivier University, 420 S. Main St., Nashua, NH 03060, USA

ARTICLE INFO

Article history:
Received 11 September 2013
Received in revised form 1 December 2013
Accepted 9 December 2013
Available online 21 December 2013

Keywords:
Anuran
Cryoprotectant
Ecogeography freeze tolerance
Glucose transport

ABSTRACT

Background: The essential role of glucose transporter 2 (GLUT2) in glucose homeostasis has been extensively studied in mammals; however, little is known about this important protein in lower vertebrates. The freeze-tolerant wood frog (*Rana sylvatica*), which copiously mobilizes glucose in response to freezing, represents an excellent system for the study of glucose transport in amphibians.
Methods: GLUT2 was sequenced from northern and southern phenotypes of *R. sylvatica*, as well as the freeze-intolerant *Rana pipiens*. These proteins were expressed and functionally characterized in *Xenopus* oocytes. Abundance of GLUT2 in tissues was analyzed using immunoblotting techniques.
Results: GLUT2s cloned from these anurans encoded proteins with high sequence homologies to known vertebrate GLUT2s and had similar transport properties, although, notably, transport of the glucose analog 3-*O*-methyl-D-glucose (3-OMG) was strongly inhibited by 150 mM urea. Proteins from all study subjects had similar affinity constants (~12 mM) and other kinetic properties; however, GLUT2 abundance in liver was 3.5-fold greater in northern *R. sylvatica* than in the southern conspecific and *R. pipiens*.
Conclusion: Our results indicate that amphibian GLUT2s are structurally and functionally similar to their homologs in other vertebrates, attesting to the conserved nature of this transport protein. The greater abundance of this protein in the northern phenotype of *R. sylvatica* suggests that these transporters contribute importantly to freezing survival.
General significance: This study provides the first functional characterization of any GLUT isoform from an anuran amphibian and novel insights into the role of these proteins in glucose homeostasis and cryoprotectant mobilization in freeze-tolerant vertebrates.

1. Introduction

One way organisms, including several terrestrially-hibernating amphibians, that overwinter in cold climates withstand the thermal challenges of winter is by tolerating the freezing of their extracellular fluid. The wood frog, *Rana sylvatica*, is one of a small group of amphibians that can survive the freezing of ~65% of its body water [1] to temperatures as low as −6 °C to −16 °C, depending on the geographic population [2]. *R. sylvatica* ranges from the state of Georgia to north of the Arctic Circle [3], and its choice of hibernaculum, beneath leaf litter in shallow depressions in the soil of the forest floor, routinely exposes it to freezing conditions, with northern populations experiencing particularly low temperatures.

Freeze tolerance is promoted by various physiological, biochemical, and molecular mechanisms; however, cryoprotectant synthesis is one of the key physiological adaptations involved in the survival of freezing [4]. Cryoprotectants contribute to freezing survival by limiting water loss, reducing ice formation, and stabilizing membranes and macromolecules [4]. In *R. sylvatica*, cryoprotective solutes accumulate gradually with the seasonal accrual of urea and rapidly with the freezing-induced mobilization of glucose; both urea and glucose contribute greatly to freezing survival [5,6]. Glucose accumulation is triggered by the initiation of freezing in peripheral tissues, causing hepatic glycogen to be converted to glucose that is quickly exported from the liver to other tissues prior to cessation of circulation [1]. Glucose improves freeze tolerance in a concentration dependent manner at the cellular, tissue, and organismal levels [6]. The glucose concentration attained in tissues during freezing is dependent on a variety of factors including the rate of glucose export from the liver, a process that requires moving glucose across cell membranes.

Transmembrane movement of glucose is mediated primarily by specialized carrier proteins, facilitative glucose transporters (GLUTs), which belong to the SLC2A gene family [7,8]. In mammals, there are thirteen known GLUT isoforms, which, based on similarities in amino acid sequence, can be grouped into three subclasses [9]. Although these isoforms are structurally similar, they differ in their tissue distribution, subcellular localization, kinetic characteristics, and regulatory

* Corresponding author at: Department of Zoology, Miami University, Oxford, OH 45056 USA. Tel.: +1 513 529 3145; fax: +1 513 529 6900.
E-mail addresses: rosendaj@miamioh.edu (A.J. Rosendale), bphilip@rivier.edu (B.N. Philip), leere@miamioh.edu (R.E. Lee), costanjp@miamioh.edu (J.P. Costanzo).

0304-4165/$ – see front matter © 2013 Elsevier B.V. All rights reserved.
http://dx.doi.org/10.1016/j.bbagen.2013.12.011

properties [10]. Glucose transporter 2 (GLUT2) is a low-affinity, high-capacity carrier that is primarily responsible for glucose transport in the liver [8]. This protein, which is known to transport various sugars including glucose, fructose, mannose, and galactose [11], has been identified in fish [12], birds [13], and mammals [7,14]. In *R. sylvatica*, carrier-mediated transport of glucose is responsible for the movement of glucose across liver membranes, and evidence suggests that evolutionary adaptation of this glucose transport system was crucial in optimizing glucose as a cryoprotectant [15,16]. Due to the importance of GLUT2 in hepatic glucose transport in other taxa, it is likely that this isoform is primarily responsible for glucose transport in the liver of *R. sylvatica*. However, the identity of this hepatic GLUT is unknown, and a full characterization of a specific GLUT isoform is lacking; in fact, a functional GLUT has yet to be characterized in any anuran.

The purpose of this study was to identify and characterize the GLUT responsible for glucose transport in the liver of *R. sylvatica* and to examine its transport kinetics in relation to cryoprotectant mobilization. To this end, we isolated and sequenced a GLUT2 homolog from *R. sylvatica*, characterized its glucose permeability, and examined its tissue distribution. This newly-identified protein was studied in a northern and southern phenotype of *R. sylvatica*, which differ in their degrees of freeze tolerance and capacity for glucose mobilization [2]. Additionally, GLUT2 was examined in the leopard frog, *Rana pipiens*, a northerly-distributed but freeze-intolerant species which also mobilizes glucose in response to freezing [17]. The functional characterization and observed differences in the abundance of hepatic GLUT2 among phenotypes/species provided novel insights into the importance of GLUTs in the evolution of freeze tolerance.

2. Materials and methods

2.1. Animals

Male *R. sylvatica* were collected from a vernal pool in southern Ohio, USA (Adams County; 38.8°N, 83.3°W) during February 2011. They were transported to our laboratory, placed inside the boxes containing damp moss, and kept in the dark at 4 °C for the next three weeks. Thereafter, they were transferred to a 48 m^2 outdoor enclosure in a wooded area of the Miami University Ecology Research Center (39.5°N, 84.7°W). Frogs were provided with a pool of water and offered crickets, dusted with a vitamin supplement (ReptoCal, Tetrafauna, Blacksburg, VA, USA), three times weekly. Feeding was supplemented with arthropods attracted to an ultraviolet-A light hung in the enclosure until feeding was suspended in late October. In November, frogs, on the verge of entering dormancy, were recaptured, brought to the laboratory, and held on damp moss in darkened boxes at 4 °C until used in January.

The northern phenotype of *R. sylvatica*, of which 6 were male and 1 was female, was collected in and around Fairbanks, Alaska, USA (64.8°N, 147.7°W) during early August, 2011. They were transported to our laboratory and housed with moist substrate in a programmable environmental chamber (Percival, model I-35X; Boone, IA, USA). Frogs were acclimatized over 5 weeks using dynamic, diel cycles of temperature and ambient light, which, based on institutional long-term records of weather, were seasonal and appropriate to the frogs' origin. Initial acclimatization temperature varied daily from 17 to 8 °C and the photophase was 16.5 h; by the end of the acclimatization in mid-September, temperature varied daily from 13 to 3 °C and the photophase was 13.3 h. Throughout the acclimatization period, frogs were fed three times weekly with vitamin-fortified crickets. Following acclimatization, frogs were kept on a moist substrate in the dark at 4 °C, until used in mid-November.

Male *R. pipiens* collected in autumn 2009 from populations in northern Minnesota were obtained commercially (Trans-Mississippi Biological Supply, Shoreview, MN, USA) in early February. They were kept at 4 °C in darkened boxes with access to dechlorinated tap water for 1 week before being used in experiments.

Frogs were euthanized by double pithing, following which aortic blood was collected into heparinized capillary tubes and plasma was isolated by centrifuging tubes at 2000 *g*. The liver, heart, brain, urinary bladder, kidney, skin, stomach, large intestine, small intestine, lung, and skeletal muscle (gracilis) were collected from Ohioan *R. sylvatica*, and liver tissue was collected from both Alaskan *R. sylvatica* and *R. pipiens*. Collected plasma and tissues were quickly frozen in liquid nitrogen and stored at −80 °C.

All experiments were conducted in compliance with the Institutional Animal Care and Use Committee at Miami University.

2.2. cDNA cloning of GLUTs

Liver samples (~100 mg) were homogenized using a shearing-type homogenizer and total RNA was extracted using Trizol (Invitrogen, Carlsbad, CA, USA) following the manufacturer's protocol. Poly(A)$^+$ mRNA was isolated from the total RNA using the PolyATract mRNA Isolation System (Promega, Madison, WI, USA) and its quality was confirmed by checking the optical density ratio at 260 nm and 280 nm [18]. cDNA was reverse-transcribed using an oligo(dT)-adaptor primer (Table 1; Integrated DNA Technologies, Coralville, IA, USA) following the manufacturer's protocol (Reverse Transcription System; Promega). The cDNA template was used in a polymerase chain reaction (PCR) using degenerate, sense (GLUT2F) and anti-sense (GLUT2R) primers designed from areas of conserved amino acid sequence from GLUT2s of various organisms, including *Homo sapiens*, *Mus musculus*, *Rattus norvegicus*, *Gallus gallus*, and *Xenopus laevis* (respective accession numbers: AAA59514, P14246, P12336, Q90592, NP_001084982). PCR was performed in 25 μl GoTaq Green Master Mix (Promega) containing 0.2 mM dNTP, 1.5 mM $MgCl_2$, 0.4 μM of each primer, 0.625 units of GoTaq DNA polymerase, and 2 μl first-strand cDNA. PCR was performed in a Veriti thermal cycler (Applied Biosystems, Foster City, CA, USA) with an initial denaturation step of 95 °C for 3 min, followed by 30 cycles of denaturation (95 °C, 1 min), annealing (54 °C, 0.5 min), and extension (72 °C, 1 min), with a final extension step of 72 °C for 10 min. A PCR product of ~500 base pair (bp) was ligated into the pGEM-T Easy plasmid cloning vector following the manufacturer's instructions (Promega), transformed into *Escherichia coli* JM109 cells, and plated on LB-ampicillin agar containing isopropyl β-D-1-thiogalactopyranoside (0.5 mM) and 5-bromo-4-chloro-3-indolyl-β-D-galactopyranoside (80 μg ml^{-1}). Plasmid DNA was isolated using High-Speed Mini Columns (IBI Scientific, Peosta, IA, USA). The sequencing reaction was performed using the BigDye Terminator v3.1 Cycle Sequencing Kit (Applied Biosystems) and standard T7 or SP6 sequencing primers (Promega). Sequences were analyzed on a 3130xl Genetic Analyzer (Applied Biosystems). Partial GLUT2 sequences were identified for each phenotype/species by comparing the obtained sequences to

Table 1
Sequences of primers used for cDNA synthesis, PCR, and sequencing.

Primer	DNA Sequence (5′–3′)	Direction
GLUT2F	CCWGTNTATGCMACYATYGGNGTIGG	Forward
GLUT2R	CTTBCCYTTNGTYTCIGGBAC	Reverse
GeneRacer RNA Oligo	CGACUGGAGCACGAGGACACUGACAU-GGGACUGAAGGAGUAGAAA	Forward
5′ RACE	CGACTGGAGCACGAGGACACTGA	Forward
5′ RACE nested	GGACACTGACATGGACTGAAGGAGTA	Forward
GLUT2 5′ GSP	TGCAGGTCGAGGACCCTGGCTGAAT	Reverse
GLUT2 3′ GSP	CAGTTTACTGGACAAGACCACAATG	Forward
3′ adaptor	GGCCACGCGTCGACTAGTAC	Reverse
Oliog(dT)-adaptor	GGCCACGCGTCGACTAGTACT (dT) $_{15}$	Reverse
GLUT2 5′ UTR SacII	AAAAAACCGCGGTCTCCAGCAGTTTAC-TGGAC	Forward
GLUT2 3′ UTR SpeI	TATAATACTAGTTTTTTTTTCATTGTTTA-CCCTGTTTAATATAACAGTCTG	Reverse
T7	TAATACGACTCACTATAGGG	Forward
SP6	TACGATTTAGGTGACACTATAG	Reverse

those published in the National Center for Biotechnology Information's (NCBI) GenBank database using nucleotide comparison (BLASTN).

To obtain full GLUT2 sequences, rapid amplification of cDNA end (RACE) techniques were used. 5′ RACE was performed by ligating the 5′ end of the mRNA with an RNA Oligo primer by following the manufacturer's instructions (GeneRacer Kit, Invitrogen). The ligated mRNA was reverse-transcribed as described above, and the resulting cDNA was used in PCR with sense primers (5′ RACE, 5′ RACE Nested) and a gene-specific (GSP), anti-sense primer (GLUT2 5′ GSP) using the PCR conditions described above, with an annealing temperature of 66 °C. 3′ RACE was performed using a sense, GSP primer (GLUT2 3′ GSP) and an anti-sense 3′ adaptor primer (Integrated DNA Technologies), with an annealing temperature of 53 °C. The 5′ RACE and 3′ RACE PCR products were cloned and sequenced as describe above. The cDNA sequences for RsOH-GLUT2, RsAK-GLUT2, and Rp-GLUT2 were submitted to GenBank (accession numbers: KF270880, KF270881, KF270882, respectively).

2.3. Analysis of sequences

DNA sequences were examined for quality in BioEdit 7.0.9.0 [19]. GLUT2 cDNA from *R. sylvatica* and *R. pipiens* were translated in silico and compared to known proteins using BLASTp with GenBank at NCBI. Hydrophobicity plots [20] were constructed using the Swiss Institute of Bioinformatics' (SIB) Expasy Proteomics server (http://web.expasy.org/protscale/) to predict the number of membrane-spanning regions, and the precise location of these transmembrane regions was confirmed using the TMHMM Server, V.2.0 (http://www.cbs.dtu.dk/services/TMHMM/). Molecular mass and isoelectric point were predicted through the Expasy server (http://web.expasy.org/compute_pi/).

Amino acid sequences of the newly-identified GLUT2s were aligned with GLUT2 proteins from *X. laevis* and *H. sapiens* using the CLUSTALW algorithm [21] in BioEdit 7.0.9.0. For phylogenetic analysis, these proteins were aligned with predicted or functionally-characterized GLUTs from other vertebrate taxa, and this alignment was imported into MEGA5 [22] for analysis. The neighbor-joining method [23] with Poisson correction and bootstrap analysis (10,000 replicates) was used to construct phylogenetic trees. Three-dimensional analysis of structural conservation among GLUTs was performed using the structural alignment of multiple proteins (STAMP) tool within the Visual Molecular Dynamics (VMD) program [24]. Percent identity was calculated for GLUT paralogs from the same phenotype/species. The alignments were colored based on their structural conservation; highly-conserved regions were colored blue, whereas red was used for regions with little or no conservation.

2.4. Xenopus oocyte preparation

For the *Xenopus* assay, plasmids were constructed containing the full-length cDNA sequences of RsOH-GLUT2, RsAK-GLUT2, and Rp-GLUT2 containing *Sac*II and *Spe*I cut sites on the 5′- and 3′-ends, respectively, by PCR using the GLUT2 5′ UTR SacII and GLUT2 3′ UTR SpeI primers (Table 1). PCR products were inserted into pGEM-T Easy plasmids containing a fragment of the *Xenopus* β-globin 5′-UTR, located downstream of the T7 promoter site and upstream of the ATG start site, as described elsewhere [25]. Cloned plasmids were linearized with *Spe*I (Invitrogen) and capped RNA (cRNA) was synthesized with the mMessage mMachine T7 Kit (Ambion, Austin, TX, USA) following the manufacturer's protocol. cRNA was treated with TURBO DNase (Ambion), recovered with MEGAclear (Ambion) purification columns and an ammonium acetate precipitation, and resuspended in RNase-free water. The cRNA from each reaction was analyzed on a Agilent 2100 Bioanalyzer (Agilent Technologies, Santa Clara, CA, USA) using the Agilent RNA 6000 Pico Kit (Agilent Technologies) and verified to contain only a single product of the expected size.

Oocytes were obtained from mature, female *X. laevis* following the protocol described by Philip et al. [25]. Briefly, ovaries were removed from double-pithed frogs, minced into small pieces, and treated with 2 mg ml^{-1} collegenase type I (Worthington Biochemical, Lakewood, NJ, USA) in Ca^{2+}-free modified Barth's solution (Ca^{2+}-free MBS; 88 mM NaCl, 1 mM KCl, 2.4 mM $NaHCO_3$, 10 mM Hepes, 0.82 mM $MgSO_4$, pH 7.5) for 3 h at 15 °C with gentle agitation. Oocytes were washed repeatedly with fresh MBS (Ca^{2+}-free MBS with 0.33 mM $Ca(NO_3)_2$, 0.41 mM $CaCl_2$; 177 mosmol kg^{-1}), and Stage V and VI oocytes were incubated overnight at 15 °C in MBS containing 10 mg l^{-1} gentamicin. Oocytes were injected using a Nanoject II injector (Drummond, Broomall, PA, USA) with 50.6 nl of 300 ng μl^{-1} cRNA or the same volume of RNase-free water. Oocytes were incubated in MBS containing 10 mg l^{-1} gentamicin for 3 d, with daily changes of media, at 15 °C before being used in assays.

2.5. Glucose transport measurements

Glucose transport kinetics in *Xenopus* oocytes expressing RsOH-GLUT2, RsAK-GLUT2, or Rp-GLUT2 were determined under zero-*trans* conditions. All transport studies used groups of 8–10 oocytes with all oocytes within a particular experimental variable (e.g., glucose uptake) coming from the same isolation/injection batch of oocytes. Transport studies were conducted at room temperature (RT; 22 °C). For basic characterization, oocytes were placed in 0.5 ml MBS containing 1 μCi 3-*O*-methyl-D-[^{3}H]glucose (3-[^{3}H]OMG; specific activity 60 Ci mM; American Radiolabeled Chemicals, St. Louis, MO, USA) and varying 3-*O*-methyl-D-glucose (3-OMG; MP Biomedicals, Santa Ana, CA, USA) concentrations (0.25, 0.5, 1, 2.5, 5, 20 mM). The reaction was terminated after 20 min by removing the radiolabelled solution and washing the oocytes three times in ice-cold phosphate buffered saline (PBS; 150 mM NaCl, 10 mM sodium phosphate, pH 7.4) containing 0.1 mM phloretin (Sigma Chemical Company, St. Louis, MO, USA), a GLUT inhibitor [26]. Oocytes were individually transferred to scintillation vials and dissolved in 0.5 ml of 1% SDS at 50 °C for 1 h. Scintillation fluid was added, and radioactivity was measured with a scintillation analyzer (Tri-Carb 2810TR; PerkinElmer, Waltham, MA, USA). The export of 3-OMG from GLUT2-expressing oocytes was measured by incubating oocytes in 0.5 ml MBS containing 3-[^{3}H]OMG/3-OMG (1 mM, 1 μCi) for 40 min. The labeled solution was completely removed, following which the oocytes were quickly washed with fresh MBS and then incubated in fresh MBS for various durations (0, 5, 10, 20, 40 min). The reaction was stopped and radioactivity was measured as described above.

To examine substrate specificity of RsOH-GLUT2, oocytes were incubated in MBS containing 50 mM of various hexoses (D- or L-glucose, galactose, mannose, and fructose; Sigma) for 30 s before 3-[^{3}H]OMG (1 μCi) was added. The reaction ran for 20 min and radioactivity was analyzed as described above. The effect of the inhibitors, phloretin (10, 50, 100 μM) and cytochalasin B (50 μM), on glucose transport was determined as described for the hexose competitors, except that 15 min was allowed prior to adding 3-[^{3}H]OMG/3-OMG.

The effect of urea on 3-OMG uptake in oocytes expressing RsOH-GLUT2, RsAK-GLUT2, and Rp-GLUT2, and urea's effect on 3-OMG export by RsOH-GLUT2-expressing oocytes was examined. For uptake studies, oocytes were incubated in MBS containing various concentrations of urea (0, 50, or 150 mM) for 30 min prior to the addition of 3-[^{3}H]OMG/3-OMG (1 mM, 1 μCi). Reactions were run for 20 min and radioactivity was analyzed as described above. For export studies, oocytes were incubated in MBS containing 3-[^{3}H]OMG/3-OMG (1 mM, 1 μCi) for 30 min. The labeled solution was completely removed, after which the oocytes were quickly washed with fresh MBS and then incubated in MBS containing 0, 50, or 150 mM urea. Reactions were stopped after 5 or 10 min and radioactivity was measured as described above. To determine if the effect of urea on 3-OMG transport was a result of the compound's colligative properties or was solute-specific, additional oocytes expressing RsOH-GLUT2 were incubated with 150 mM acetone

or glycerol, and 3-OMG uptake was measured as described for the urea uptake studies.

For each experiment, 3-OMG transport mediated by the GLUT2 proteins was calculated by subtracting the average 3-OMG concentration obtained for corresponding sham-injected oocytes.

2.6. Immunoblots

The abundance of GLUT2 in the liver, heart, brain, urinary bladder, kidney, skin, stomach, large intestine, small intestine, lung, and skeletal muscle (gracilis) of Ohioan *R. sylvatica*, as well as the liver from Alaskan *R. sylvatica* and *R. pipiens*, was examined by immunoblotting. Tissues were homogenized in STE buffer (250 mM NaCl, 10 mM Tris–HCl, pH 8.3, 5 mM EDTA) containing a protease-inhibitor cocktail (Sigma) using a shearing-type homogenizer. The homogenate was centrifuged at 1000 *g* for 10 min at 4 °C, and the resulting supernatant was centrifuged at 16,000 *g* for 20 min at 4 °C. The pellet was resuspended in STE buffer, aliquoted, and frozen at −80 °C. Final protein concentration was determined using the Bio-Rad (Bradford) protein assay (Bio-Rad, Hercules, CA, USA) with bovine serum albumin (BSA) as a standard. Protein (20 μg) samples were mixed with Laemmli sample buffer (Bio-Rad) containing 5% β-mercaptoethanol, incubated for 10 min at RT, and analyzed by immunoblotting and densitometry techniques as previously described [27]. To verify that the same amount of protein was loaded in all lanes and that transfer was equivalent across the gels, membranes were stained with 0.2% (w/v) Ponceau S (Sigma) containing 5% acetic acid. Membranes were digitally scanned and total protein was analyzed by densitometry (as previously described [27]) for GLUT2 normalization. An oligopeptide corresponding to a C-terminus region of the ranid GLUT2 (Cys–EFRKKKHGGKKSTEMEY) was used to develop a polyclonal GLUT2 antibody in rabbit (Proteintech, Chicago, IL, USA). The rabbit serum was affinity-purified (SulfoLink Immobilization Kit; Pierce Protein Research Products, Rockford, IL, USA) and used in immunoreactions at a final concentration of 0.2 μg ml^{-1} in TBS-T containing 5% non-fat milk. To check specificity, the anti-GLUT2 antibody was exposed to a molar excess of its antigenic peptide in a competition assay. Additionally, the antibody was used to probe *Xenopus* oocytes expressing RsOH-GLUT2, RsAK-GLUT2, and Rp-GLUT2. Oocytes were homogenized in STE buffer with protease inhibitors, and the oocyte proteins were probed with the anti-GLUT2 antibody (0.2 μg ml^{-1}).

2.7. Statistical analyses

Results are shown as means ± 1 SEM. Glucose uptake kinetics were compared among GLUT2 proteins using non-linear regression with the Prism (GraphPad, La Jolla, CA, USA) Michaelis–Menten model, $Y = V_{max} * X / (K_m + X)$, or linear regression, where appropriate. The overall trend in glucose export was compared using non-linear regression with the Prism exponential one-phase decay model ($Y = (Y_0 - \text{Plateau}) * \exp(-K * X) + \text{Plateau}$). A two-way ANOVA with a Tukey post hoc test was used to compare glucose export at specific time points, as well as the effect of urea on 3-OMG uptake. A one-way ANOVA with a Tukey post hoc test was used to analyze the effect of inhibitors and various hexoses on 3-OMG transport, as well as differences in the abundance of GLUT2 in the liver among phenotypes/species. Data obtained for the effect of acetone or glycerol on 3-OMG uptake and the effect of urea on 3-OMG export in RsOH-GLUT2-expressing oocytes did not meet assumptions of parametric analysis, thus they were analyzed by a Kruskal–Wallis test with a Dunn post hoc test. For certain experiments, data are represented in figures as groups normalized to control, to better represent fold changes; however, all statistical analyses were performed on raw (non-normalized) data. Means were considered significantly different at $P < 0.05$.

3. Results

3.1. Isolation, cloning, and sequencing of ranid GLUT2s

cDNA sequences with high homology to mammalian GLUT2 were obtained for Ohioan and Alaskan phenotypes of *R. sylvatica*, and *R. pipiens*, using degenerate primers designed against conserved regions of vertebrate GLUT2s. Each full sequence (1609 bp) contained a 1491 bp open-reading frame (Genbank accession numbers KF270880, KF270881, KF270882), and in silico translated cDNA revealed proteins consisting of 497 amino acids (Fig. 1A), with predicted molecular masses of 53.9 kDa and isoelectric points of 8.96. One putative N-glycosylation site was identified for each protein at amino acid 58; additionally, various motifs were conserved among functional GLUTs. Hydropathy analysis of each protein predicted 12 transmembrane regions with the N and C termini positioned in the cytoplasm (Fig. 1). The predicted three-dimensional structures of the three proteins, compared using the VMD program, demonstrated a high degree of structural similarity to each other (*Q*-values >0.95). Additionally, they had a high degree of structural conservation, predominately in the transmembrane helices, when compared to other vertebrate GLUT2s (Fig. 1B).

The three proteins shared a high degree of identity (>95%) among each other. When compared to other taxa, they showed the highest degree of amino acid identity with their GLUT2 homolog in *Xenopus tropicalis* (82%) and *X. laevis* (81%), although these ranid proteins also shared identity with mammalian GLUT2s (~60%). Phylogenetic analysis to determine the relatedness of the three newly-characterized GLUT2s to other vertebrate GLUTs demonstrated that these transporters grouped with the predicted GLUT2 for *X. laevis* and were more similar to GLUT2 than the other GLUT isoforms (Fig. 2). Therefore, the deduced protein sequences from *R. sylvatica* and *R. pipiens* were considered ranid orthologs of GLUT2.

3.2. Functional characterization

The presence of conserved motifs among the amino acid sequences of the newly-identified GLUT2s and other functional GLUT2s suggested that RsOH-GLUT2, RsAK-GLUT2, and Rp-GLUT2 are functional GLUT2 proteins. However, to confirm this prediction, exogenous GLUT2s were translated in *Xenopus* oocytes and glucose transport across the oocyte membrane was measured under zero-trans conditions using the glucose analog, 3-*O*-methyl-D-glucose (3-OMG). The rate of uptake of 3-OMG occurred in a dose-dependent manner in oocytes expressing RsOH-GLUT2, RsAK-GLUT2, and Rp-GLUT2 (Fig. 3A), demonstrating that these are functional glucose transporters. Using a nonlinear regression analysis of the transport data, K_m values for RsOH-GLUT2, RsAK-GLUT2, and Rp-GLUT2 were 11.1 ± 2.3, 12.3 ± 2.6, and 11.9 ± 2.5, respectively, and did not differ among the groups ($F = 0.07$, $P = 0.94$). V_{max} values also did not differ ($F = 0.12$, $P = 0.89$) among RsOH-GLUT2 (617 ± 61), RsAK-GLUT2 (660 ± 69), and Rp-GLUT2 (627 ± 66). To verify that the calculated transport kinetics did not vary among proteins, 3-OMG uptake was linearized by inversely transforming the transport data, and kinetics were determined using a Lineweaver–Burk plot (Fig. 3B). There was no difference among the slopes ($F = 2.45$, $P = 0.13$) or Y intercepts ($F = 1.54$, $P = 0.25$), confirming transport kinetics did not differ among the three proteins.

To determine if glucose transport was bidirectional, and if the rate of glucose export differed among *Xenopus* oocytes expressing RsOH-GLUT2, RsAK-GLUT2, or Rp-GLUT2, we measured the movement of 3-OMG out of oocytes. 3-OMG entered the oocytes during a 40 min incubation in a solution containing 3-OMG (1 mM); oocytes were then transferred to a 3-OMG-free solution and incubated for various durations to measure 3-OMG export. There was a time-dependent transport of 3-OMG from the oocytes (Fig. 3C); however, the overall export of 3-OMG did not differ ($F = 0.04$, $P = 0.96$)

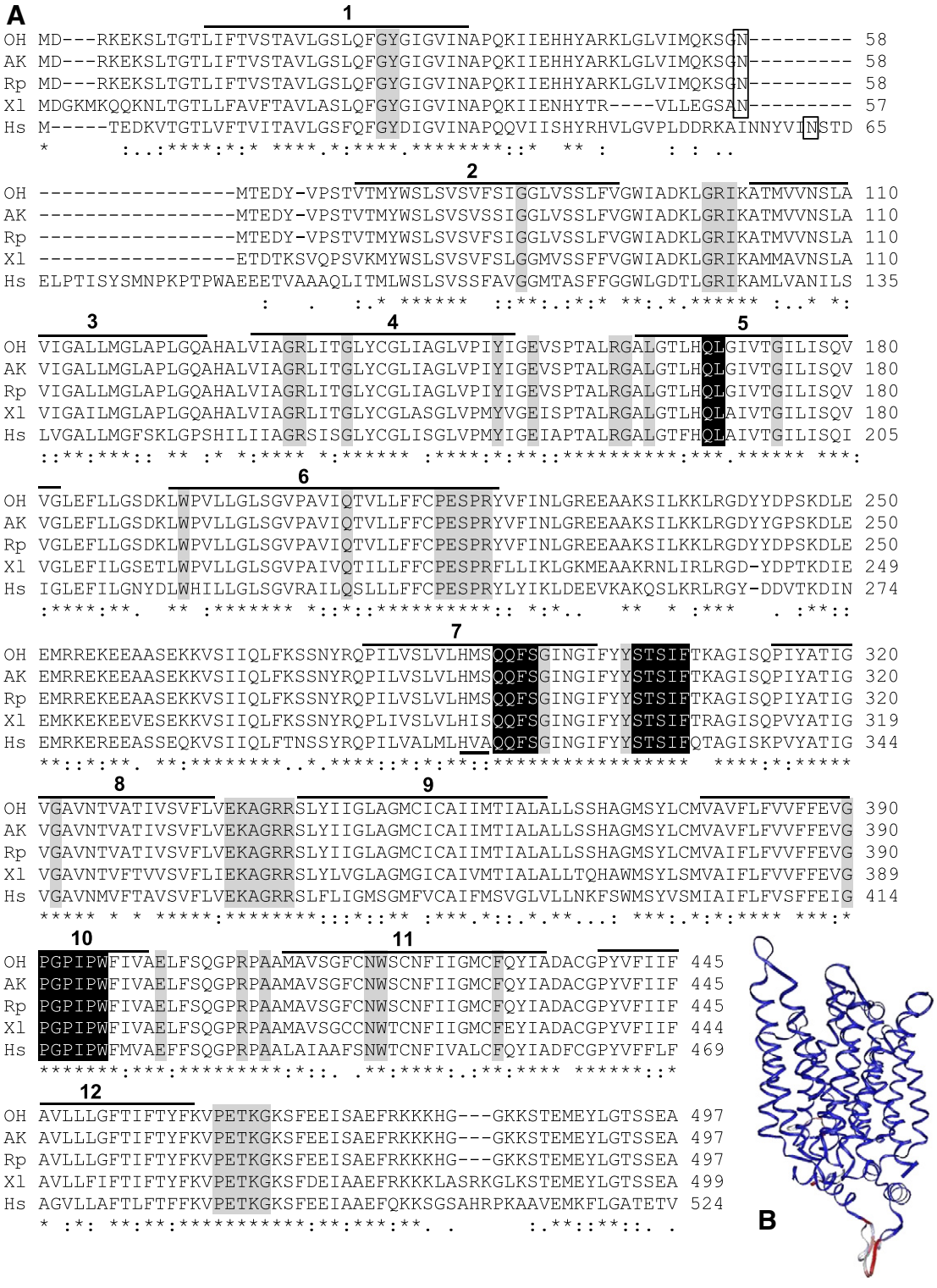

Fig. 1. Sequences of newly-identified, ranid glucose transporter 2 (GLUT2) in relation to GLUTs known from other taxa. A: Deduced amino acid sequences of newly-identified GLUT2s from Ohioan *Rana sylvatica* (OH), Alaskan *R. sylvatica* (AK), and *R. pipiens* (Rp), aligned with GLUT2 from *Xenopus laevis* (Xl; accession no. NP_001084982) and *Homo sapiens* (Hs; accession no. NP_000331) using ClustalW in BioEdit v7.0.9.0. Gaps in the amino acid sequences are indicated with a dash (–). Amino acids that are identical (*), highly conserved (:), or moderately conserved (.) among all five sequences are identified. Box highlights a putative N-glycosylation site; horizontal bars and numbers indicate the putative 12 transmembrane regions. Amino acids that are specific to members of class 1 glucose transporters are highlighted with black; residues conserved among all GLUTs are highlighted with gray; and the HVA motif characteristic of mammalian GLUT2 is underlined [9]. B: Three-dimensional ribbon model of ranid GLUT2s, *X. laevis* GLUT2, and *H. sapiens* GLUT2 demonstrating structural alignment of multiple proteins (STAMP) tool within the Visual Molecular Dynamics (VMD) program. Structurally-conserved regions (blue) were found primarily within the membrane-spanning regions; whereas, less structural conservation (red) was found in the connecting loops.

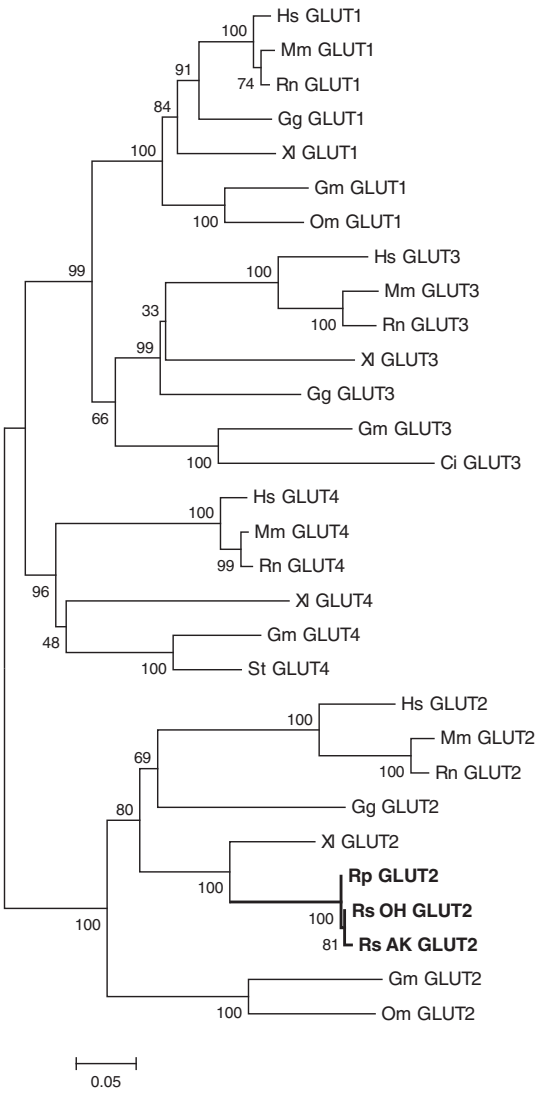

Fig. 2. Phylogenetic tree demonstrating the relationships among the newly-identified, functional ranid GLUT2s, Ohioan *Rana sylvatica* (Rs OH), Alaskan *R. sylvatica* (Rs AK), and *R. pipiens* (Rp); and functionally-characterized and/or predicted GLUTs from other vertebrates including *Homo sapiens* (Hs), *Mus musculus* (Mm), *Rattus norvegicus* (Rn), *Gallus gallus* (Gg), *Xenopus laevis* (Xl), *Gadus morhua* (Gm), *Oncorhynchus mykiss* (Om), *Ctenopharyngodon idella* (Ci), and *Salmo trutta* (St). Accession numbers: *H. sapiens* GLUT1 (AAA52571), *M. musculus* GLUT1 (AAA37752), *R. norvegicus* GLUT1 (P11167), *G. gallus* GLUT1 (AAB02037), *X. laevis* GLUT1 (NP_001088068), *O. mykiss* GLUT1 (AAF75681), *G. morhua* GLUT1 (AAS17880), *H. sapiens* GLUT2 (AAA59514), *M. musculus* GLUT2 (P14246), *R. norvegicus* GLUT2 (P12336), G. gallus GLUT2 (Q90592), *X. laevis* GLUT2 (NP_001084982), *O. mykiss* GLUT2 (AAK09377), *G. morhua* GLUT2 (AAV63984), *R. sylvatica* OH GLUT2 (KF270880), *R. sylvatica* AK (KF270881), *R. pipiens* (KF270882), *H. sapiens* GLUT3 (AAB61083), *M. musculus* GLUT3 (AAH34122), *R. norvegicus* GLUT3 (Q07647), *G. gallus* GLUT3 (AAA48662), *X. laevis* GLUT3 (NP_001079713), *C. idella* GLUT3 (AAP03065), *G. morhua* GLUT3 (AAT67456), *H. sapiens* GLUT4 (AAA59189), *M. musculus* GLUT4 (P14142), *R. norvegicus* GLUT4 (P19357), *X. laevis* GLUT4 (NP_001085607), *S. trutta* GLUT4 (AAG12191), and *G. morhua* GLUT4 (AAZ15731). The tree was constructed using the neighbor-joining method with Poisson correction. The number of substitutions per amino acid site is represented in the scale bar. Bootstrap proportions (10,000 replicates) are indicated above the nodes.

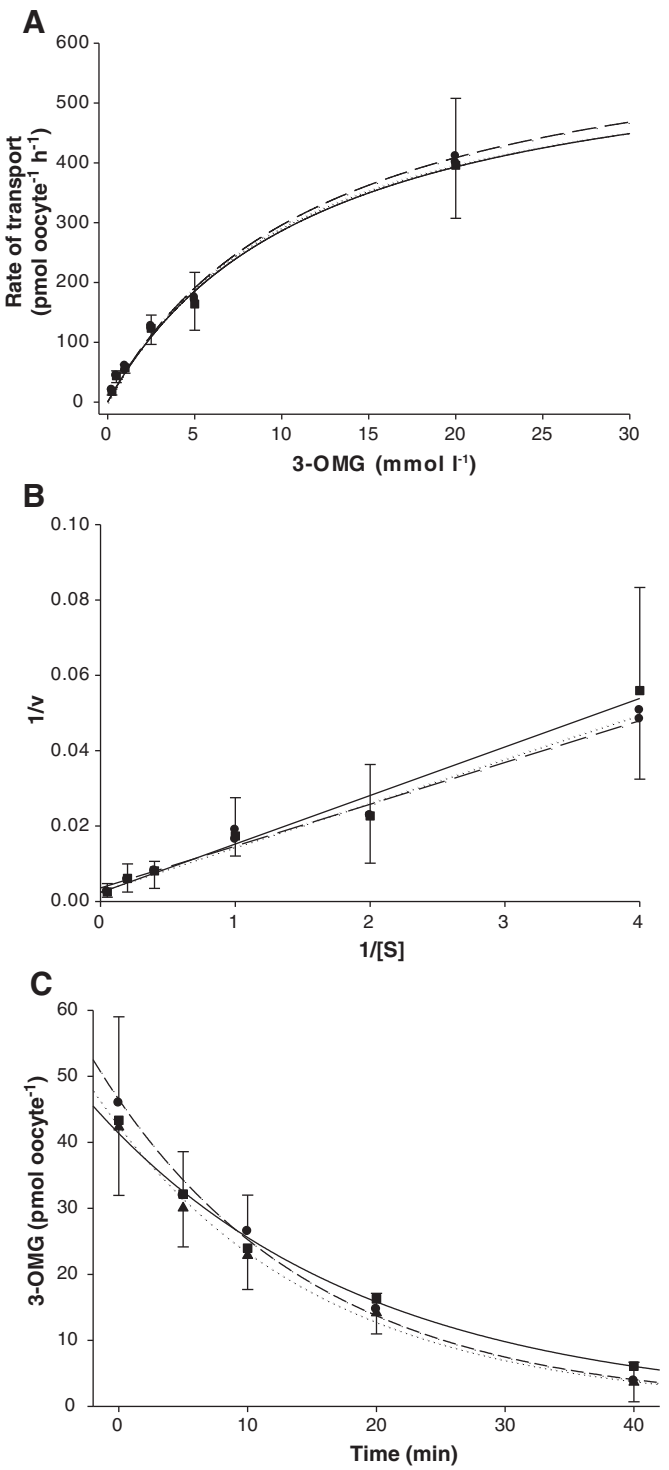

Fig. 3. Kinetics of glucose transport in *Xenopus* oocytes expressing RsOH-GLUT2 (▲, dashed line), RsAK-GLUT2 (●, dotted line), or Rp-GLUT2 (■, solid line). Prior to the assay, oocytes were injected with 50 nl of GLUT2 cRNA (300 ng μl^{-1}). A: 3-O-methyl-D-glucose (3-OMG) uptake measured under zero-*trans* conditions at various 3-OMG concentrations. Uptake values reflect measured 3-OMG concentrations minus average values obtained for respective sham-injected oocytes. B: Lineweaver–Burk plot from the linearization of data acquired in zero-*trans* kinetic studies. Values are means ± SEM. (n = 8–10 oocytes). C: 3-OMG export was measured under zero-*trans* conditions at various times. Export values reflect measured 3-OMG concentrations minus average values obtained for respective sham-injected oocytes. Values are means ± SEM (n = 8–10 oocytes).

among RsOH-GLUT2, RsAK-GLUT2, and Rp-GLUT2, nor were there any differences among the proteins at any of the time points ($F = 0.10$, $P = 0.90$).

The effect of transporter inhibitors and various sugars on 3-OMG uptake was determined by exposing RsOH-GLUT2-expressing oocytes to these substances prior to performing 3-OMG uptake assays. Various inhibitors and sugars had a significant ($F = 19.9$, $P < 0.0001$) effect on 3-OMG transport. Phloretin inhibited 3-OMG transport in a concentration-dependent manner (Fig. 4A), with 0.05 mM and 0.1 mM decreasing uptake by 51% ($P < 0.01$) and 96% ($P < 0.001$), respectively. Cytochalasin B also inhibited RsOH-GLUT2, inducing

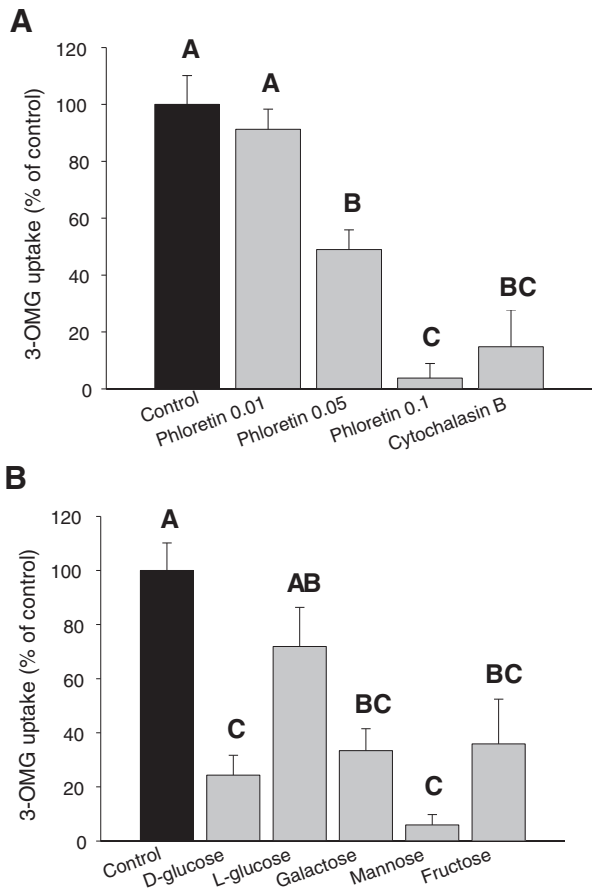

Fig. 4. Inhibition of 3-O-methyl-D-glucose (3-OMG) uptake in *Xenopus* oocytes injected with RsOH-GLUT2 cRNA. A: Inhibition of 3-OMG uptake in RsOH-GLUT2-expressing oocytes pre-incubated with phloretin or cytochalasin B. B: Substrate-specificity of Rs-GLUT2 assessed by competition assay with D- and L-glucose, galactose, mannose, and fructose. Uptake of 3-OMG is expressed as a percentage of uptake into oocytes incubated without inhibitors or hexoses. Uptake values reflect measured 3-OMG concentrations minus average values obtained for respective sham-injected oocytes. Values are means ± SEM (n = 8–10 oocytes). Letters that differ from one another indicate significant differences between group means ($P < 0.05$).

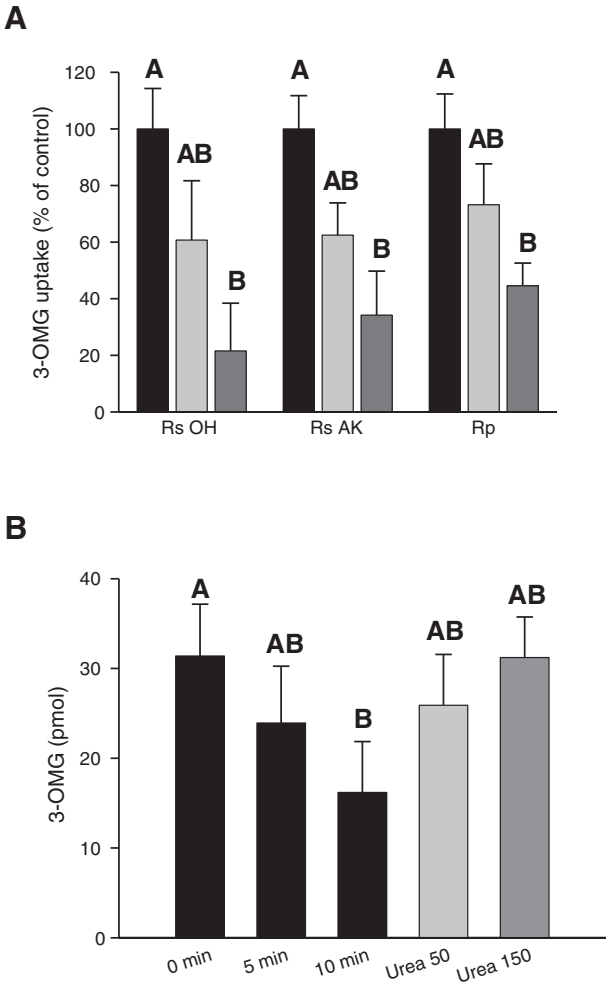

Fig. 5. Effect of urea on 3-O-methyl-D-glucose (3-OMG) transport in *Xenopus* oocytes injected with RsOH-GLUT2, RsAK-GLUT2, or Rp-GLUT2 cRNA. A: Inhibition of 3-OMG uptake by urea. Oocytes were preincubated with 0 mM (black bars), 50 mM (gray bars), or 150 mM (dark gray bars) urea prior to 3-OMG uptake experiments. Uptake of 3-OMG is expressed as a percentage of uptake into oocytes incubated without urea. B: Inhibition of 3-OMG export by urea in oocytes expressing RsOH-GLUT2. Oocytes were pre-incubated with 3-OMG, then transferred to MBS containing 0 mM (black bars), 50 mM (gray bars), or 150 mM (dark gray bars) urea for 0, 5, or 10 min. 3-OMG values reflect measured 3-OMG concentrations minus average values obtained for respective sham-injected oocytes. Values are means ± SEM (n = 8–10 oocytes). Mean values identified by different letters were statistically distinguishable ($P < 0.05$).

an 85% decrease ($P < 0.001$) in 3-OMG uptake. Inhibition of 3-OMG uptake was also induced by pre-incubation with several sugars (Fig. 4B), including D-glucose (76%), galactose (67), mannose (94%), and fructose (64%; $P < 0.001$ for all cases). However, L-glucose did not affect 3-OMG uptake ($P > 0.05$), suggesting stereospecificity of this transporter.

To determine the effect of urea on the function of RsOH-GLUT2, RsAK-GLUT2, and Rp-GLUT2, oocytes expressing these proteins were pre-incubated with 0, 50, or 150 mM urea prior to performing 3-OMG transport experiments. Urea concentration had an overall effect on GLUT2 function ($F = 14.3$, $P < 0.0001$); however, the effect of urea did not vary among phenotypes/species ($F = 0.11$, $P = 0.98$). Pre-incubation with 150 mM urea decreased 3-OMG uptake in RsOH-GLUT2 ($P < 0.05$), RsAK-GLUT2 ($P < 0.01$), and Rp-GLUT2 ($P < 0.01$) expressing oocytes by 55–65% (Fig. 5A). Urea also inhibited 3-OMG export; oocytes expressing RsOH-GLUT2, pre-incubated with 50 or 150 mM urea, showed no significant decrease in 3-OMG content after 10 min incubation in MBS (Fig. 5B). To determine if the observed inhibition by urea was solute-specific or rather the result of colligative effects, RsOH-GLUT2-expressing oocytes were pre-incubated with 150 mM acetone or glycerol prior to performing 3-OMG transport experiments. 3-OMG values (pmol) for oocytes pre-incubated with acetone (19.6 ± 6.6) or glycerol (20.0 ± 3.6) did not differ ($H = 0.36$, $P = 0.84$) from control (23.5 ± 7.5).

3.3. Tissue distribution and hepatic abundance of GLUT2

Following characterization of the structure and function of RsOH-GLUT2, RsAK-GLUT2, and Rp-GLUT2, we examined the tissue distribution of RsOH-GLUT2 in Ohioan *R. sylvatica* and compared the abundance of these proteins in liver tissue from all phenotypes/species. We used a polyclonal antibody against a portion of the ranid GLUT2 corresponding to amino acids 474–490 towards the C-terminus. The antibody was verified to react with GLUT2 by probing protein isolated from RsOH-GLUT2, RsAK-GLUT2, and Rp-GLUT2 cRNA-injected *Xenopus* oocytes and confirming that the antibody reacted with cRNA-injected, but not sham-injected oocytes (Fig. 6A). Immunoblots probed with the anti-GLUT2 antibody resulted in a single band at 54 kDa, which corresponded to the in silico predicted molecular mass.

Tissues from Ohioan *R. sylvatica* probed with the anti-GLUT2 antibody showed variable abundance of the protein (Fig. 6B). When standardized to total protein, GLUT2 was detected in high abundance in the liver and brain, at intermediate levels in the heart, kidney, and small and large intestine, and trace amounts in the bladder, skin, lung,

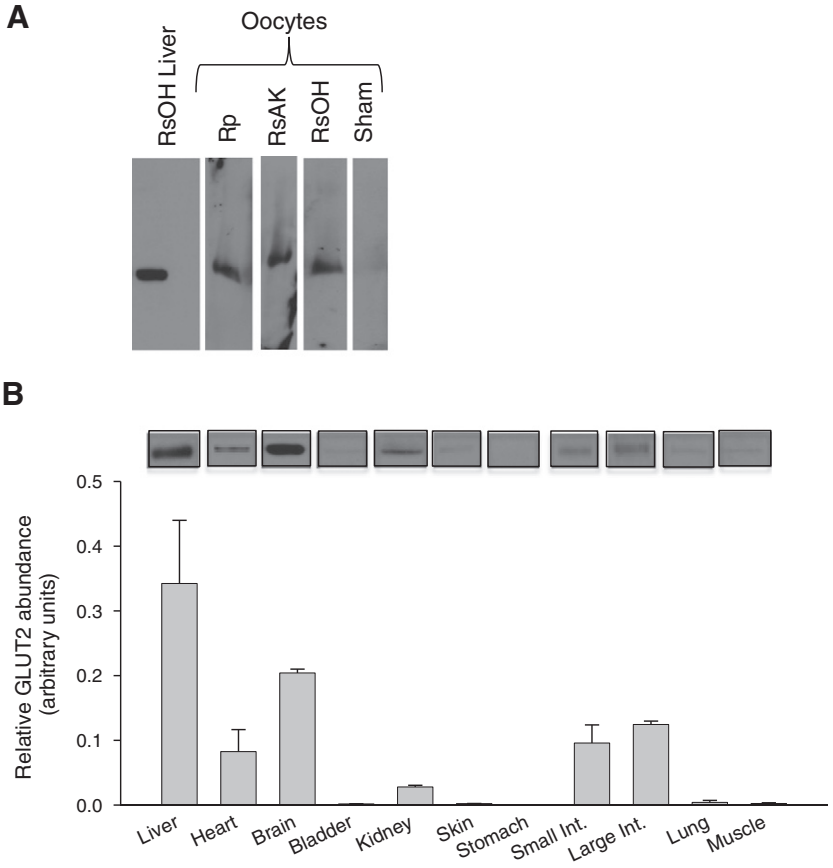

Fig. 6. Tissue distribution of GLUT2 protein from Ohioan *Rana sylvatica* examined by immunoblotting. A: Immunoblot of GLUT2 protein in Ohioan *R. sylvatica* liver using an antibody (Ab) designed against the ranid GLUT2; a single band was detected at 54 kDa. Ab specificity was confirmed by probing *Xenopus* oocytes injected with RsOH-GLUT2 (RsOH), RsAK-GLUT2 (RsAK), Rp-GLUT2 (Rp) cRNA, or nuclease-free water (sham). B: Select immunoblots of tissues (20 μg protein) probed with the anti-GLUT2 antibody, showing immunoreactive bands at 54 kDa (bands not intended to show relative abundance). Relative abundance of GLUT2 protein, standardized to total protein, among tissues was determined by densitometry. Intensity values are mean ± SEM (n = 6).

and skeletal muscle. GLUT2 was not detected in the stomach. Comparison of GLUT2 abundance in liver among Ohioan *R. sylvatica*, Alaskan *R. sylvatica*, and *R. pipiens* showed that GLUT2 varied among phenotypes/species ($F = 18.7$, $P < 0.0001$). GLUT2 was ~3.5-fold more abundant in liver of Alaskan frogs than Ohioan *R. sylvatica* ($P < 0.001$) and *R. pipiens* ($P < 0.001$) (Fig. 7). There was no difference in GLUT2 abundance in liver between Ohioan *R. sylvatica* and *R. pipiens* ($P > 0.05$).

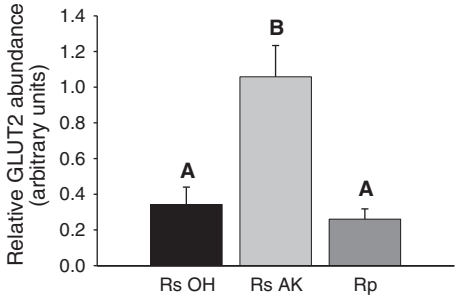

Fig. 7. Relative abundance of GLUT2 protein in the liver of Ohioan *Rana sylvatica* (Rs OH), Alaskan *R. sylvatica* (Rs AK), and *R. pipiens* (Rp) determined by immunoblotting. Tissues (20 μg protein) were probed with an antibody designed against the ranid GLUT2 and relative abundance of GLUT2 protein, standardized to total protein, was determined by densitometry. Intensity values are mean ± SEM (n = 6). Different letters indicate significant differences among groups ($P < 0.001$).

4. Discussion

One of the mechanisms underpinning freezing survival in ectotherms is the accumulation of cryoprotective solutes. In *R. sylvatica*, this involves the prehibernal accrual of urea and the freezing-induced synthesis and distribution of glucose from the liver. The movement of glucose across hepatic membranes of *R. sylvatica* is carrier mediated [15,16] and likely involves one or more GLUT isoforms. To clarify the mechanisms of glucose transport, we identified, functionally characterized the glucose permeability, determined the tissue distribution, and compared hepatic abundance of a GLUT2 homolog from two phenotypes of the freeze-tolerant *R. sylvatica*, and the freeze-intolerant *R. pipiens*. Our results help to elucidate the role of these proteins in freezing survival and their possible contributions to cryoprotectant mobilization.

4.1. Sequence and phylogenetic analysis of ranid GLUT2s

Novel GLUT2 proteins identified in *R. sylvatica* and *R. pipiens* were similar in sequence, predicted topology, and function to previously-characterized GLUTs. RsOH-GLUT2, RsAK-GLUT2, and Rp-GLUT2 all contained 12 membrane-spanning regions, which is characteristic of GLUTs [10]. Additionally, various amino acids implicated as being functionally important were conserved in these novel proteins. The proline-rich region GPGPIP in helix 10, which is found in all GLUTs, was present in our proteins; additionally, the GR(R/K) motif, which is important in conformation changes during transport, was also present [10].

Characteristic of other GLUT2s, the QLS motif found in high-affinity GLUTs [28–30] was absent from the ranid GLUT2s. The absence of these amino acids, coupled with the presence of the H(V/M)A motif in helix 7, has been implicated in fructose transport in mammalian GLUTs [29]; however, unlike mammalian GLUT2s, the H(V/M)A motif was only partially conserved in the ranid GLUT2s. In mammalian GLUT2, the proline-rich region of helix six, which is present in most GLUTs, is modified with most prolines being substituted for other amino acids [30]. In contrast, only one of those prolines (P213F) was replaced in the ranid GLUT2.

In addition to the presence of evolutionarily-conserved motifs, overall amino acid identity was high among the newly-identified proteins and predicted amphibian (~80%) and characterized mammalian GLUT2s (~60%). The amino acid identity was reflected in the high degree of structural similarity shared among these proteins, which was especially evident in the transmembrane regions responsible for forming the aqueous pore, through which glucose passes [29].

Phylogenetic analysis of RsOH-GLUT2, RsAK-GLUT2, and Rp-GLUT2 revealed that these proteins group with other GLUT2s, forming a distinct clade separate from other GLUT isoforms. Not surprisingly, the ranid GLUT2s grouped with the predicted GLUT2 sequence from *X. laevis*, forming an amphibian GLUT2 clade. Of note, the amphibian GLUT2s aligned more closely with the avian and mammalian proteins than with fish GLUT2s, potentially reflecting changes in this protein during vertebrate evolution.

4.2. Functional characterization of ranid GLUT2s

Examination of the sugar transport properties of RsOH-GLUT2, RsAK-GLUT2, and Rp-GLUT2 demonstrated unequivocally that these proteins are functional glucose transporters. These proteins, when expressed in *Xenopus* oocytes, showed affinity constants (K_m) for the glucose analog 3-OMG of ~12 mM. The 3-OMG K_m values for these ranid GLUT2s were lower than the 30–40 mM observed for mammalian GLUT2 [7]; however, the latter values were obtained using the equilibrium-exchange method of measuring transport kinetics, and the zero-trans kinetics method used in this study tends to result in lower K_m and V_{max} values for GLUTs [28] Our K_m values were very similar to those observed for 2-deoxy-D-glucose transport in fish (11 mM) and mammals (11–16) under zero-trans conditions [7,12,31]. Glucose transport examined under equilibrium-exchange conditions in hepatic membranes isolated from *R. sylvatica* demonstrated a K_m of 30–60 mM [15,16], further suggesting that our low K_m values were a result of experimental conditions and not inherent properties of the proteins themselves.

An unexpected outcome of our identification of the functional GLUT2s was the discovery of sequences that were highly similar (~85%) to the characterized ranid GLUT2s. These sequences coded for proteins of 499 amino acids and preliminary analysis suggested that these proteins may be GLUT2 paralogs, referred to hereafter as RsOH-GLUT2B, RsAK-GLUT2B, Rp-GLUT2B (accession numbers KF270883, KF270884, KF270885). These proteins were expressed in the *Xenopus* oocytes and glucose transport across the oocyte membrane was measured in the same manner as RsOH-GLUT2, RsAK-GLUT2, and Rp-GLUT2. However, these proteins did not transport 3-OMG under our experimental conditions (data not shown). Therefore, further characterization experiments were only conducted on the functional RsOH-GLUT2, RsAK-GLUT2, and Rp-GLUT2. Further study of these proteins is necessary to determine what, if any, role these proteins play in glucose homeostasis.

K_m and V_{max} values did not differ between phenotypes or species, suggesting that neither glucose affinity nor transport capacity of GLUT2 has changed during the evolution of freeze tolerance in these frogs. There were relatively few amino acid differences among RsOH-GLUT2, RsAK-GLUT2, and Rp-GLUT2, indicating that this protein has been well conserved among the phenotypes/species; likely more substantial changes in the protein sequence would be necessary to elicit changes in transport kinetics. Due to the consumptive nature of the glucose transport assays, we could not quantify GLUT2 protein abundance in the oocytes used in the assays; therefore, we must assume that equal loading of cRNA resulted in equal GLUT2 abundance in the oocyte membranes. Nevertheless, qualitative analysis of oocytes injected with GLUT2 cRNA but not used in transport assays indeed indicated similar GLUT2 protein abundance occurred among oocytes (Fig. 6A). Our results support the findings of King et al. [15] who compared carrier-mediated transport of glucose in isolated hepatic membranes of *R. sylvatica* and *R. pipiens* and found that the transport kinetics did not differ between those species.

In oocytes expressing RsOH-GLUT2, phloretin and cytochalasin B, the classic extracellular and intracellular inhibitors of glucose transport, respectively, reduced 3-OMG uptake in a dose-dependent manner. Analyses of competitive inhibition by various hexoses demonstrated that RsOH-GLUT2 had a substrate specificity similar to that observed for both fish and mammalian GLUT2s [11,12,31], allowing the transport of D-glucose, galactose, mannose, and fructose, but not L-glucose. These findings further demonstrate the similar biochemical properties of the ranid GLUT2s with previously-characterized GLUT2s and support observations that the transport properties of GLUT2 have been well conserved throughout vertebrate evolution [12].

Exogenous substances like phloretin and cytochalasin B have been extensively studied as GLUT inhibitors; however, inhibition of glucose transport by endogenous metabolites has received less attention, and, as far as we know, our data are the first direct evidence of the inhibitory effect of urea on a specific GLUT isoform. In *R. sylvatica*, urea seasonally accumulates in tissues and body fluid, and urea levels can reach 50 to more than 200 mM in fall and early winter, depending on the population and environmental conditions [2,5]. In addition to its cryoprotective effects, urea is known to affect activity of certain enzymes [32] and to depress overall metabolism of some dormant ectotherms, including *R. sylvatica* [33,34]. In RsOH-GLUT2, RsAK-GLUT2, and Rp-GLUT2 expressing-oocytes, urea inhibited glucose influx and efflux in a dose-dependent manner, although the mechanism of inhibition was not determined. Two glucose transporters, GLUT9 and SGLT1, have been implicated in the transport of nitrogenous wastes such as uric acid and urea [35], respectively, but it is unclear if urea transport also occurs through ranid GLUT2s, potentially causing the observed inhibition. Urea is not transported through GLUTs in isolated erythrocytes [36]; instead, urea acts as a non-transportable competitive inhibitor, likely by binding to the substrate site [36]. Inhibition of glucose transport has also been observed in erythrocytes exposed to urea analogs, such as thiourea [37]. The lack of inhibition by glycerol and acetone, solutes with relatively low and high membrane permeability, respectively, indicates that the inhibitory effect of urea and its analogs was solute specific. Urea's effect on GLUT functioning appears to occur at relatively high concentrations, only affecting ranid GLUT2 at >50 mM urea in our tests. *R. sylvatica* routinely accumulates urea to the inhibitory levels observed in our study; therefore, the inhibitory effect of urea on glucose transport is likely physiologically relevant in *R. sylvatica*.

Urea's inhibition of GLUT2 provides a possible explanation to a physiological phenomenon observed in overwintering *R. sylvatica*. Following a freezing event, glucose mobilized from the liver and accumulated in tissues throughout the body is reabsorbed in the liver and reconverted to glycogen [1,4]. However, winter-acclimatized Alaskan *R. sylvatica*, which have relatively high levels of plasma urea (~100 mM) remain hyperglycemic at least 5 d post-thaw [2]. Similarly, hyperglycemia persists 24 h post thaw in frogs experimentally urea-loaded prior to freezing [38]. Delayed glucose uptake into the liver by urea-inhibited GLUT2 could account for this persistent hyperglycemia. The implications of delayed glucose clearance remain unclear; however, this post-freeze hyperglycemia may be beneficial in fueling repair processes and/or supplementing cryoprotectant levels during subsequent freezing exposures [39].

4.3. Tissue distribution and hepatic abundance of ranid GLUT2s

The variation in cellular metabolism and glucose requirements among tissues necessitates multiple tissue-specific GLUT isoforms, each with different regulatory and kinetic properties [10]. In mammals, GLUT2 is commonly referred to as the liver-type GLUT, but is also found predominately in small intestine, pancreas, and kidney [14]. Similar to mammals, *R. sylvatica* uses glucose to meet energetic requirements; however, the need to rapidly distribute glucose among tissues during freezing, for which the high-capacity kinetics of GLUT2 are ideally suited, may necessitate a more diverse distribution of this transporter. Using an antibody designed against ranid GLUT2, we found that, as in mammals, RsOH-GLUT2 was most abundant in the liver. Hepatic GLUT2 plays an important role in the bidirectional transport of glucose in hepatocytes [10], a process that is critical to survival of *R. sylvatica* during freezing and subsequent thawing [4]. RsOH-GLUT2 was also highly abundant in brain, where GLUT2 is thought to play a role in glucose sensing and regulation of energy homeostasis [40]. In conjunction with sodium-glucose transporters (SGLTs), GLUT2 functions in small and large intestine for sugar absorption following meals [14,41]; RsOH-GLUT2 likely also plays a role in nutrient absorption in these tissues. GLUT2s also function cooperatively with SGLTs in the kidney, where renal reabsorption of glucose occurs [14]. In *R. sylvatica*, GLUT2 could contribute to reabsorption of glucose in the kidney and urinary bladder, a process critical in preventing loss of glucose through excretion following a freezing event [4]. Although GLUT4 has traditionally been considered the main glucose transporter in cardiac and skeletal muscle, recent studies have detected GLUT2 mRNA in these tissues [12,42]; our detection of GLUT2 protein in heart and gracilis supports the idea that GLUT2 may play a role in glucose transport in frog cardiac and skeletal muscle. RsOH-GLUT2 was detected at low levels in the lung and skin, both tissues where GLUT2 expression has been shown [10,12], but was not detected in the stomach where other GLUT isoforms are responsible for glucose transport [43].

The cryoprotectant system of freeze-tolerant anurans demands a timely export of newly synthesized glucose from the hepatocyte into the bloodstream. Accordingly, an earlier study [15] demonstrated that the capacity to transport glucose across the liver plasma membrane is greater in *R. sylvatica* than in a closely related, but freeze-intolerant species, *R. pipiens*. Our finding that GLUT2 was substantially more abundant in the liver of *R. sylvatica* (albeit not in the southern phenotype) as compared to *R. pipiens* corroborates this earlier result. Alaskan *R. sylvatica* are exposed to lower winter temperatures in their hibernacula as compared to their southern counterparts [44], and their smaller body size [2,3] confers them with reduced thermal capacitance, potentially limiting the time available to distribute cryoprotectant. Conceivably, the 3.5-fold greater abundance of GLUT2 we found in this phenotype as compared to Ohioan frogs could help mitigate this liability. Taken together, these results suggest GLUT2 plays an important role in the freezing adaptation of anurans.

4.4. Conclusions

In this study, we identified and characterized a GLUT2 homolog from *R. sylvatica* and *R. pipiens* and considered the implications of this protein in the evolution of anuran freeze tolerance. Alaskan *R. sylvatica* can tolerate freezing to temperatures 10–12° Celsius lower than their Ohioan counterparts and *R. pipiens* is a freeze-intolerant species, yet there was no difference in transport kinetics of glucose by GLUT2 among these animals. On the other hand, Alaskan *R. sylvatica* maintained a greater abundance of GLUT2 in the liver and thus, all else being equal, had a superior capacity to rapidly mobilize glucose. This is clearly a potential benefit to their cryoprotectant system [39], although to some extent the greater abundance of GLUT2 may serve only to counteract the inhibitory levels of urea that these frogs can accrue [2]. Besides its role in exporting cryoprotectant from the liver, GLUT2 likely mediates glucose uptake in the various other tissues in which it occurs. Unlike other GLUT isoforms that become saturated at physiological levels of glucose, GLUT2 maintains transport at high concentrations [11], thereby facilitating the rapid accumulation of glucose in tissues during freezing. This property is especially beneficial to organs such as the brain and heart, both of which accumulate high levels of glucose during freezing [2] and have a relatively high abundance of GLUT2. Overall, the results of this study suggest that GLUT2 plays an important role in glucose homeostasis and cryoprotectant distribution in frogs, and that this protein may have contributed to the evolution of freeze tolerance in anurans that utilize glucose as a cryoprotectant.

Acknowledgments

We thank Brian Barnes for sharing his knowledge on the biology of Alaskan wood frogs. We thank Don Larson and David Russell for assisting in the logistical aspects of collecting frogs in Alaska. Alice Reynolds provided technical assistance. Clara do Amaral assisted in frog collections, provided technical assistance, and, along with two anonymous reviewers, contributed constructive comments on the manuscript. We thank Paul James for assistance with the experiments utilizing radioactive isotopes. This work was supported by the National Science Foundation [IOS1022788 to J.P.C.].

References

[1] K.B. Storey, J.M. Storey, Physiology, biochemistry, and molecular biology of vertebrate freeze tolerance: the wood frog, in: E. Benson, B. Fuller, N. Lane (Eds.), Life in the Frozen State, CRC Press, Washington, DC, 2004, pp. 243–274.
[2] J.P. Costanzo, M.C. Do Amaral, A.J. Rosendale, R.E. Lee Jr., Hibernation physiology, freezing adaptation and extreme freeze tolerance in a northern population of the wood frog, J. Exp. Biol. 216 (2013) 3461–3473.
[3] B.S. Martof, R.L. Humphries, Geographic variation in the wood frog *Rana sylvatica*, Am. Midl. Nat. 61 (1959) 350–389.
[4] J.P. Costanzo, R.E. Lee Jr., Avoidance and tolerance of freezing in ectothermic vertebrates, J. Exp. Biol. 216 (2013) 1961–1967.
[5] J.P. Costanzo, R.E. Lee Jr., Cryoprotection by urea in a terrestrially hibernating frog, J. Exp. Biol. 208 (2005) 4079–4089.
[6] J.P. Costanzo, R.E. Lee Jr., P.H. Lortz, Glucose concentration regulates freeze tolerance in the wood frog *Rana sylvatica*, J. Exp. Biol. 181 (1993) 245–255.
[7] J.E. Pessin, G.I. Bell, Mammalian facilitative glucose transporter family: structure and molecular regulation, Annu. Rev. Physiol. 54 (1992) 911–930.
[8] A.R. Manolescu, K. Witkowska, A. Kinnaird, T. Cessford, C. Cheeseman, Facilitated hexose transporters: new perspectives on form and function, 22 (2007) 234–240.
[9] H.G. Joost, B. Thorens, The extended GLUT-family of sugar/polyol transport facilitators: nomenclature, sequence characteristics, and potential function of its novel members, Mol. Membr. Biol. 18 (2001) 247–256.
[10] N. Gorovits, M.J. Charron, What we know about facilitative glucose transporters: lessons from cultured cells, animal models, and human studies, Biochem. Mol. Biol. Educ. 31 (2003) 163–172.
[11] G.W. Gould, H.M. Thomas, T.J. Jess, G.I. Bell, Expression of human glucose transporters in *Xenopus* oocytes: kinetic characterization and substrate specificities of the erythrocyte, liver, and brain isoforms, Biochemistry 30 (1991) 5139–5145.
[12] J. Castillo, D. Crespo, E. Capilla, M. Díaz, F. Chauvigne, J. Cerda, J.V. Planas, Evolutionary structural and functional conservation of an ortholog of the GLUT2 glucose transporter gene (SLC2A2) in zebrafish, Am. J. Physiol. Regul. Integr. Comp. Physiol. 297 (2009) R626–R632.
[13] M.Y. Wang, M.Y. Tsai, C. Wang, Identification of chicken liver glucose transporter, Arch. Biochem. Biophys. 310 (1994) 172–179.
[14] B. Thorens, H.K. Sarkar, H.R. Kaback, H.F. Lodish, Cloning and functional expression in bacteria of a novel glucose transporter present in liver, intestine, kidney, and beta-pancreatic islet cells, Cell 55 (1988) 281–290.
[15] P.A. King, M.N. Rosholt, K.B. Storey, Adaptations of plasma membrane glucose transport facilitate cryoprotectant distribution in freeze-tolerant frogs, Am. J. Physiol. 265 (1993) R1036–R1042.
[16] P.A. King, M.N. Rosholt, K.B. Storey, Seasonal changes in plasma membrane glucose transporters enhance cryoprotectant distribution in the freeze-tolerant wood frog, Can. J. Zool. 73 (1995) 1–9.
[17] J.P. Costanzo, R.E. Lee Jr., P.H. Lortz, Physiological responses of freeze-tolerant and-intolerant frogs: clues to evolution of anuran freeze tolerance, Am. J. Physiol. 265 (1993) R721–R725.
[18] K.L. Manchester, Use of UV methods for measurement of protein and nucleic acid concentrations, Biotechniques 20 (1996) 968–970.
[19] T.A. Hall, BioEdit: a user-friendly biological sequence alignment editor and analysis program for Windows 95/98/NT, Nucleic Acids Symp. Ser. 41 (1999) 95–98.
[20] J. Kyte, R.F. Doolittle, A simple method for displaying the hydropathic character of a protein, J. Mol. Biol. 157 (1982) 105–135.

[21] J.D. Thompson, D.G. Higgins, T.J. Gibson, CLUSTAL W: improving the sensitivity of progressive multiple sequence alignment through sequence weighting, position-specific gap penalties and weight matrix choice, Nucleic Acids Res. 22 (1994) 4673–4680.
[22] K. Tamura, D. Peterson, N. Peterson, G. Stecher, M. Nei, N.L. Trottier, MEGA5: molecular evolutionary genetics analysis using maximum likelihood, evolutionary distance, and maximum parsimony methods, Mol. Biol. Evol. 28 (2011) 2731–2739.
[23] N. Saitou, M. Nei, The neighbor-joining method: a new method for reconstructing phylogenetic trees, Mol. Biol. Evol. 4 (1987) 406–425.
[24] W. Humphrey, A. Dalke, K. Schulten, VMD: visual molecular dynamics, J. Mol. Graph. (1996) 33–38.
[25] B.N. Philip, A.J. Kiss, R.E. Lee, The protective role of aquaporins in the freeze-tolerant insect *Eurosta solidaginis*: functional characterization and tissue abundance of EsAQP1, J. Exp. Biol. 214 (2011) 848–857.
[26] R.M. Krupka, Evidence for a carrier conformational change associated with sugar transport in erythrocytes, Biochemistry 10 (1971) 1143–1148.
[27] A.J. Rosendale, J.P. Costanzo, R.E. Lee Jr., Seasonal variation and response to osmotic challenge in urea transporter expression in the dehydration- and freeze-tolerant wood frog, *Rana sylvatica*, J. Exp. Zool. 317A (2012) 401–409.
[28] S.A. Baldwin, Mechanisms of active and passive transport in a family of homologous sugar transporters found in both prokaryotes and eukaryotes, in: J. de Pont (Ed.), J.J.H.H.M. De Pont (Ed.), Molecular Aspects Of Transport Proteins, New York, 1992, pp. 169–217.
[29] M.P. Barrett, A.R. Walmsleyt, G.W. Gould, Structure and function of facultative sugar transporters, Curr. Opin. Cell Biol. 11 (1999) 496–502.
[30] G.I. Bell, T. Kayano, J.B. Buse, C.F. Burant, J. Takeda, D. Lin, H. Fukumoto, S. Seino, Molecular biology of mammalian glucose transporters, Diabetes Care 13 (1990) 198–208.
[31] C.A. Colville, M.J. Seatter, T.J. Jess, G.W. Gould, H.M. Thomas, Kinetic analysis of the liver-type (GLUT2) and brain-type (GLUT3) glucose transporters in *Xenopus* oocytes: substrate specificities and effects of transport inhibitors, Biochem. J. 290 (1993) 701–706.
[32] K.J. Cowan, K.B. Storey, Urea and KCl have differential effects on enzyme activities in liver and muscle of estivating versus nonestivating species, Biochem. Cell Biol. 80 (2002) 745–755.
[33] T.J. Muir, J.P. Costanzo, R.E. Lee Jr., Evidence for urea-induced hypometabolism in isolated organs of dormant ectotherms, J. Exp. Zool. 313A (2010) 28–34.
[34] T.J. Muir, J.P. Costanzo, R.E. Lee Jr., Osmotic and metabolic responses to dehydration and urea-loading in a dormant, terrestrially hibernating frog, J. Comp. Physiol. B. 177 (2007) 917–926.
[35] L. Bankir, B.X. Yang, New insights into urea and glucose handling by the kidney, and the urine concentrating mechanism, Kidney Int. 81 (2012) 1179–1198.
[36] R.M. Krupka, Inhibition of sugar transport in erythrocytes by fluorodinitrobenzene, Biochemistry 10 (1971) 1148–1153.
[37] R.R. Mayrand, D.G. Levitt, Urea and ethylene glycol-facilitated transport systems in the human red cell membrane. Saturation, competition, and asymmetry, J. Gen. Physiol. 81 (1983) 221–237.
[38] J.P. Costanzo, M. Marjanovic, E.A. Fincel, R.E. Lee Jr., Urea loading enhances post-freeze performance of frog skeletal muscle, J. Comp. Physiol. B. 178 (2008) 413–420.
[39] J.P. Costanzo, R.E. Lee Jr., M.F. Wright, Cooling rate influences cryoprotectant distribution and organ dehydration in freezing wood frogs, J. Exp. Zool. 261 (1992) 373–378.
[40] B. Thorens, A gene knockout approach in mice to identify glucose sensors controlling glucose homeostasis, Pflügers Arch. Eur. J. Phys. 445 (2003) 482–490.
[41] N.P. Taylor, R. Manjarin, A.D. Woodward, Transcript profiles of hexose transporters in the equine gastrointestinal tract, J. Equine Vet. Sci. 32 (2012) 346–351.
[42] J.J. Zuo, Z.Y. Huang, A.M. Zhi, S.G. Zou, X.Y. Zhou, F.W. Dai, D.Y. Feng, Cloning and distribution of facilitative glucose transporter (SLC2A2) in pigs, Asian Aust. J. Anim. 23 (2010) 1159–1165.
[43] T. Yoshikawa, R. Inoue, M. Matsumoto, T. Yajima, K. Ushida, T. Iwanaga, Comparative expression of hexose transporters (SGLT1, GLUT1, GLUT2 and GLUT5) throughout the mouse gastrointestinal tract, Histochem. Cell Biol. 135 (2011) 183–194.
[44] L.B. Middle, B.M. Barnes, Overwintering strategies of the wood frog, *Rana sylvatica*, in interior Alaska, Am. Zool. 40 (2000) 1132–1133.